

Recent advances in numerical modeling of catalytic monolith reactors

Steffen Tischer*, Olaf Deutschmann

Institute for Chemical Technology and Polymer Chemistry, University of Karlsruhe, 76128 Karlsruhe, Germany

Abstract

This work focuses on the development and improvement of numerical tools for the simulation of catalytic monolith reactors. These simulations cover detailed descriptions of reaction mechanisms, transport in gas-phase and washcoats, fluid flow in single channels, and the entire reactor. In DETCHEM^{MONOLITH}, the concept of building a transient model of the monolith reactor by the calculation of steady-state solutions of representative channels has been improved. Thus, simulations with inlet conditions varying in space and time become feasible. Furthermore, reactors with alternating channel properties can be considered. Another extension concerns storage catalysts that accounts for transient surface coverages of the storage medium.

As example, three numerical studies are shown: a catalytic combustion device with alternating active and inactive channels, a catalytic combustion monolith with spatially varying inlet conditions, and a NO_x storage catalyst with alternating inlet conditions.

© 2005 Elsevier B.V. All rights reserved.

Keywords: Catalytic monolith reactors; Numerical modeling; NO_x storage

1. Introduction

Catalytic monolith reactors have numerous applications in industrial processes and as technical devices. Since our previous publication [1], one focus is set especially on automotive catalytic converters [2–5]. Although, they are used successfully to reduce the vehicles' emissions for more than two decades, they still remain a very complex system from the modeling viewpoint. However, further improvements in the reduction of emissions depend on a sound understanding of the interaction between chemical and physical processes inside the converter. Complexities arise, for instance, from continuously changing inlet conditions that require a transient description of the entire reactor. Detailed numerical simulations are a useful tool to verify the models. The validated models then will assist in the further improvement of catalytic converters and the development of new after-treatment strategies. A good summary of recent modeling approaches for automotive catalytic converters has been written by Pontikakis et al. [5].

In this context, catalytic devices with oxygen or NO_x storage components have received considerable attention recently [6–9]. Whereas for the classic systems, the time scales of the catalytic processes are usually much smaller than the thermal response times of the reactor, we now also must consider storage reactions and heat balance simultaneously.

Another important application of catalytic monolith reactors is their use as combustion stage for gas turbines leading to reduced NO_x formation. However, today's catalysts will not resist the high temperatures if all the fuel is burnt catalytically. As a solution, the catalytic burner is only used in the first combustion stage. In order to avoid overheating, the monolith consists of alternating catalytic active and inactive channels [10].

2. Numerical model

The computer program DETCHEM^{MONOLITH} [1,11] has been extended in order to be capable of simulating a larger variety of systems. It applies hierarchically arranged detailed models from an atomic scale up to reactor scale.

* Corresponding author. Tel.: +49 721 608 6715; fax: +49 721 608 4805.
E-mail address: tischer@ict.uni-karlsruhe.de (S. Tischer).

Nomenclature

c_p	heat capacity ($\text{J kg}^{-1} \text{K}^{-1}$)
d	distance function
\dot{H}_{gas}	integral enthalpy flux in gas phase (J s^{-1})
q_{H}	heat source term ($\text{J m}^{-3} \text{s}^{-1}$)
t	time (s)
T	temperature (K)
u	axial velocity (m s^{-1})
w^k	weight
x_i	spatial vector (m)
x^k	input vector for clustering
Y_i	mass fraction

Greek letters

δT	temperature difference for normalization (K)
$\delta \Theta$	coverage difference for normalization
Θ	surface coverage
λ_{ij}	heat conduction tensor ($\text{W m}^{-1} \text{K}^{-1}$)
ξ_u	relative velocity difference for normalization
ξ_Y	relative difference in mass fractions for normalization
ρ	density (kg m^{-3})
σ	channel density (m^{-2})
Φ_{H}	heat flux (W m^{-2})

The core is a library for the description of species properties based on atomistic models and for reactions among gas-phase and surface species based on elementary-step reaction mechanisms. It provides interfaces for the calculation of thermodynamic properties and transport coefficients of gas-phase species. Individual surface types can be defined to represent different types of catalysts, each of which is assigned an individual microscopic surface site density and macroscopic surface area. It is important to note the difference between these two surface parameters, because only the microscopic surface site density influences the rates of surface reactions, whereas the macroscopic surface area scales the net fluxes in the interaction with the gas phase. Diffusion in washcoats can be accounted for either by solving a set of reaction–diffusion equations or by applying an effectiveness-factor model.

Under a quasi steady-state assumption, the fluid flow in each channel is described by either a 1D plug-flow with transport limitation model or a 2D boundary-layer approach with detailed transport models [1,12]. For given inlet and wall conditions, the resulting differential–algebraic equation systems are solved using a semi-implicit Euler method with extrapolation by the solver LIMEX [13].

Individual channels are combined into a transient temperature model for the monolithic bulk. The temperature field of the monolith is treated as a homogeneous continuum in one, two or three dimensions. The only restriction for the geometry of the monolith is that the shape of the cross-

section does not change along the (axial) direction of the channels. The evolution of the transient temperature field T can be written as¹:

$$\rho c_p \frac{\partial T}{\partial t} = - \frac{\partial}{\partial x_i} \Phi_{\text{H},i} + q_{\text{H}} \quad (1)$$

where ρ is the effective density of the monolith, c_p the specific heat capacity, Φ_{H} the heat flux vector, and q_{H} is the heat source term (due to interaction with gas-phase). The diffusive heat flux inside the monolith is modeled by anisotropic heat conduction

$$\Phi_{\text{H},i} = - \lambda_{ij} \frac{\partial T}{\partial x_j} \quad (2)$$

where the heat conduction coefficient λ can take different values for the axial and radial directions. The modeled reactor may consist of several layers with different material properties to account for insulation, etc. All properties are functions of temperature. A fixed temperature or arbitrary heat fluxes including terms for conduction, convection, or radiation can be defined as boundary conditions. The heat source terms are calculated during the simulation of the gas-phase flow through the channels. The heat transfer from the gas-phase into the solid or vice versa is indicated by a change of the integral enthalpy flux \dot{H}_{gas} in the gas phase:

$$q_{\text{H}} = - \sigma \frac{\partial \dot{H}_{\text{gas}}}{\partial x_1} \quad (3)$$

The channel density σ denotes the number of channels per unit area of the cross-section. Since the numerical simulation of the fluid flow is the most time consuming step, not every possible channel is simulated in detail.

Due to the representation of the monolith by a discrete grid, there is a unique channel wall temperature profile for each axial row of grid points. Furthermore, when applying spatially varying inlet conditions, the channels may differ in inlet temperature T , velocity u , and species mass fractions Y_1, \dots, Y_s . However, this finite number of variables completely defines the parameters for a channel simulation, i.e. the calculation of source terms can be viewed as a mapping from the input vector

$$x^k = (T_{\text{wall},1}^k, \dots, T_{\text{wall},n}^k, T_{\text{in}}^k, u_{\text{in}}^k, Y_{\text{in},1}^k, \dots, Y_{\text{in},s}^k) \quad (4)$$

of the k th discretized channel to an output vector containing the q_{H} of the respective grid points. This mapping can be expected to be continuous – channels with similar input vectors may result in similar source terms. For the identification of similar channels an agglomerative cluster algorithm is applied [14].

A weight w^k can be assigned to each vector x^k that accounts for the absolute number of channels represented by x^k , which is proportional to the size of the corresponding monolith grid cell. In addition, we need a distance function

¹ Einstein convention: implicit summing over indices that appear twice.

$d(x^i, x^j)$ for which a normalized maximum norm was chosen:

$$d(x^i, x^j) = (d_T(T_{\text{wall},1}^i, T_{\text{wall},1}^j), \dots, d_T(T_{\text{wall},n}^i, T_{\text{wall},n}^j), \\ d_T(T_{\text{in}}^i, T_{\text{in}}^j), d_u(u_{\text{in}}^i, u_{\text{in}}^j), d_Y(Y_{\text{in},1}^i, Y_{\text{in},1}^j), \dots, \\ d_Y(Y_{\text{in},s}^i, Y_{\text{in},s}^j)) \quad (5)$$

with distance functions

$$d_T(T^i, T^j) = \frac{|T^i - T^j|}{\delta T} \quad (6)$$

$$d_u(u^i, u^j) = \frac{|u^i - u^j|}{\xi_u \max(u^i, u^j)}, \text{ and} \quad (7)$$

$$d_Y(Y^i, Y^j) = \frac{|Y^i - Y^j|}{\xi_Y \max(Y^i, Y^j)} \quad (8)$$

Temperatures are normalized with respect to a temperature difference δT , whereas inlet velocities and mass fractions are normalized by their relative deviations ξ_u and ξ_Y , respectively.

The agglomerative cluster algorithm, illustrated in Fig. 1, can be sketched as follows:

1. Find the minimum $d^* = d(x^{i^*}, x^{j^*}) = \min_{i \neq j} (d(x^i, x^j))$.
2. If $d^* > 1$ then stop.

3. Let $x^* = (w^{i^*} x^{i^*} + w^{j^*} x^{j^*}) / (w^{i^*} + w^{j^*})$ and $w^* = w^{i^*} + w^{j^*}$.
4. Eliminate (x^{i^*}, w^{i^*}) , (x^{j^*}, w^{j^*}) and replace by (x^*, w^*) .
5. Go to 1.

The remaining x^k are the input vectors for representative channels. All input vectors in one cluster are associated with the same output source terms. Since the channel equations are not explicitly time dependent, the number of channel calculations can be further reduced by including the x^k of previously calculated channels into the clustering and reusing their results.

The simulation method can further be extended to storage catalysts. For this type of catalysts, the surface coverages of the storage medium are not in steady-state during the single channel simulation. If we also assume a separation of time scales between the fast catalytic reactions and the slow storage reactions, the coverages can be included in the monolith model. Together with the monolith temperature and the inlet conditions they become part of the input vector x^k when calling the channel simulation, which in return passes the gas-phase concentrations at the gas–solid boundary to the monolith. The transient coverages of the storage medium are then calculated along with the temperature field. During clustering, a distance function

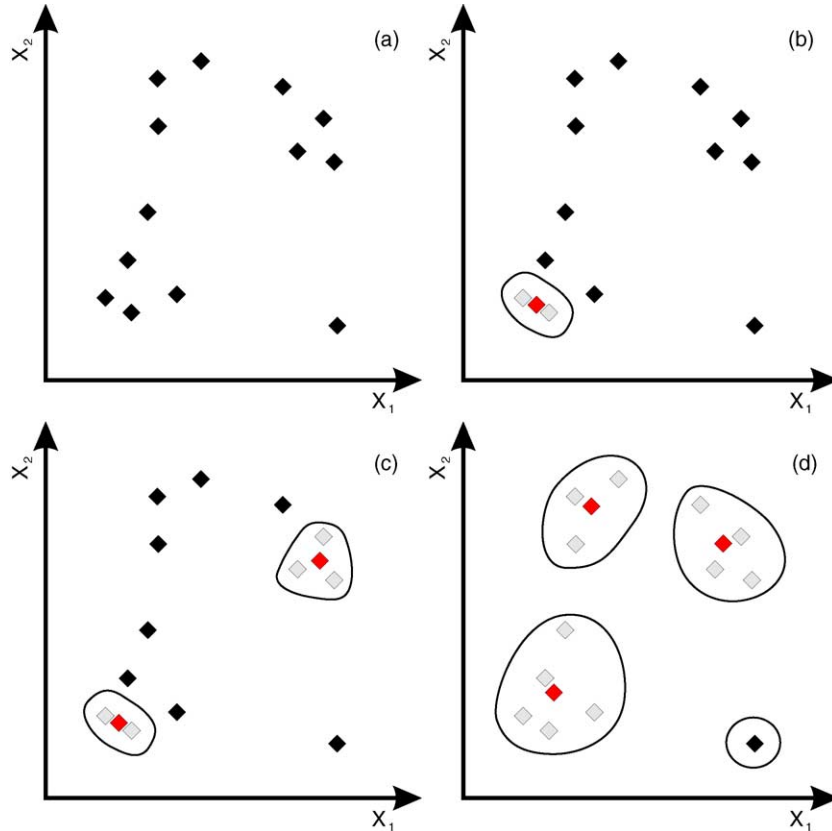


Fig. 1. Agglomerative cluster algorithm. (a) Given set of data points. (b) Join two data points into one cluster. (c) After the third agglomeration step two clusters have been formed. (d) Final representation of the data by four clusters.

with normalization with respect to an absolute coverage difference $\delta\Theta$ is used:

$$d_{\Theta}(\Theta^i, \Theta^j) = \frac{|\Theta^i - \Theta^j|}{\delta\Theta} \quad (9)$$

Since the single channel simulation is treated as a black-box process in the monolith simulation, the same input vector could be used to call more than one channel simulation in order to calculate the heat source terms. The channels can, for instance, differ in size and surface properties as long as the different channel types are arranged regularly and the continuum model is still applicable. It is also possible to simulate counter-flow configurations with this approach.

3. Catalytic combustion monoliths

The first system that shall be studied is a catalytic combustion stage for a gas turbine. One problem arising in the technical application is that the catalysts used are only stable up to temperatures of 800–900 °C, whereas temperatures at the entrance of the turbine can be as high as 1300 °C. Therefore, catalytic combustors are only considerable as a first combustion stage.

If a stoichiometric methane/air mixture entering at 298 K is burnt, the resulting adiabatic temperature is as high as 2239 K [15]. Although under non-adiabatic conditions the temperature is significantly lower, it is still too high for a catalytic process. The temperature could be reduced by reducing the amount of fuel in the catalytic stage, but remixing the rest of the fuel with the hot products is also not desirable. An idea to avoid these problems is to cool the catalytic reactor with unburnt gases. Therefore, a monolithic reactor can be built in a way where only every second channel is catalytically active.

Such a system shall be studied numerically. Assume a cylindrical cordierite monolith ($\lambda_{\text{axial}} = 2.5 \text{ W m}^{-1} \text{ K}^{-1}$, $\lambda_{\text{radial}} = 1.5 \text{ W m}^{-1} \text{ K}^{-1}$, $\rho = 2100 \text{ kg m}^{-3}$, $c_p = 850 \text{ J kg}^{-1} \text{ K}^{-1}$) 30 cm long and 20 cm in diameter. It shall contain channels at a density of 400 cpsi, whereas in one case all of the channels are coated with platinum and in the other case coated and uncoated channels alternate. In the coated channels, the total active catalytic surface equals the geometrical surface area of the channel wall. The initial temperature of the monolith was set to 1000 K. The stoichiometric methane/air mixture entered the monolith with a velocity of 2 m/s at a temperature of 298 K and pressure of 1 bar. As boundary condition, radiation with an emissivity of 0.8 was assumed. The catalytic reactions on platinum were modeled by 27 irreversible reactions among nine gas-phase and 11 surface species [16].

Fig. 2 shows the comparison of the simulated temperatures between the two cases. In both cases, a steady-state solution is reached after approximately 150 s. The gas exit

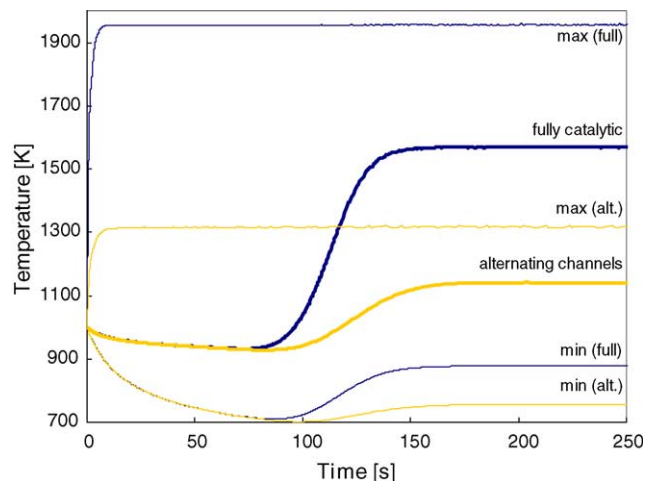


Fig. 2. Simulated transient monolith (min/max) and gas-phase exit temperatures for catalytic combustion monoliths with fully coated and with alternatingly coated channels.

temperatures are 1570 K for the fully coated monolith and 1140 K for the monolith with alternating channels. More important for the stability of the catalyst is the maximum temperature in the solid. It reaches 1955 and 1320 K, respectively. The maximum is reached within the first 10 s after ignition. Although the cold incoming gases can cool down the monolith in the beginning, the reaction zone is spreading towards the entrance in time. Although the maximum temperature in the case of the alternating channels is still too high by about 100 K, this simple model shows the applicability of the numerical tool. In real world applications, one could decrease the fuel content or increase the heat conductivity of the monolith to lower the peak temperatures.

4. Inhomogeneous inlet profiles

A two-dimensional model of the monolith is not always sufficient. Under the assumption of homogeneous inlet conditions, the most influential parameter for the temperature profile of the channel is the normal distance of the channel from the exterior wall of the monolith. However, this homogeneity may sometimes not be guaranteed in a technical application [17]. In the case of automotive catalytic converters, for instance, it is known that an inhomogeneous inlet profile has a negative impact on the conversion during cold start [18]. Such a system can be studied numerically with a three-dimensional model of the monolith. As an example, the ignition of catalytic combustion is chosen.

Again we consider a cylindrical cordierite monolith with a diameter of 24 and 10 cm in length and a channel density of 400 cpsi. In order to compare a homogeneous and an inhomogeneous inlet profile, two cases were simulated. In both cases, the mean inlet velocity was $v_0 = 0.416 \text{ m/s}$ at a temperature of 300 K. The inhomogeneous profile was

constructed by an anti-symmetric function:

$$v(y, z) = v_0 \left[1 + 0.9 \sin \left(\frac{y}{r} \pi \right) \left(1 - \frac{y^2 + z^2}{r^2} \right) \right] \quad (10)$$

The profile is illustrated in Fig. 3. An inlet gas composition of 2.75% methane with 17.25% oxygen in nitrogen dilution was chosen. The monolith wall temperature was increased by 5 K/min to simulate the influence of an external heating. The initial temperature of 500 K is low enough in order to establish a temperature profile inside the monolith before ignition occurs.

The grid of the monolith was discretized by 30 cells in axial, 9 cells in radial and 12 cells in circumferential direction. With clustering parameters $\delta T = 10$ K and $\xi_u = 0.1$, a maximum of 23 channels had to be simulated for the homogeneous profile; and between 15 and 69 channels were chosen for the inhomogeneous profile. However, by reusing results from previous channels, hardly more than 10 channels were simulated in one iteration time step.

If one wants to evaluate the efficiency of the combustion process, one can look at the global methane conversion (Fig. 4). Although the ignition starts earlier for the inhomogeneous profile, the integral conversion is lower in that case. The reason for this behaviour is the fact that ignition occurs first in the channels with a lower mass flow. The cooling by the incoming cold gas is less efficient. However, the heat released by the combustion is not sufficient to increase the temperature of the channels with higher flow rates. The latter ones have a higher weight in the determination of the net conversion and therefore conversion is low until ignition occurs there.

These arguments can be verified when looking at the temperature field of the inhomogeneous case (Fig. 5). After 60 min a quasi steady-state temperature profile has been established. The incoming gases cool down the monolith.

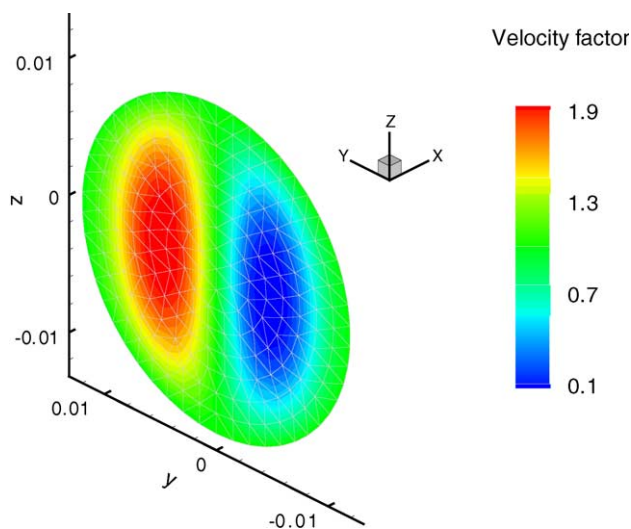


Fig. 3. Normalized velocity distribution of the monolith with inhomogeneous inlet profile.

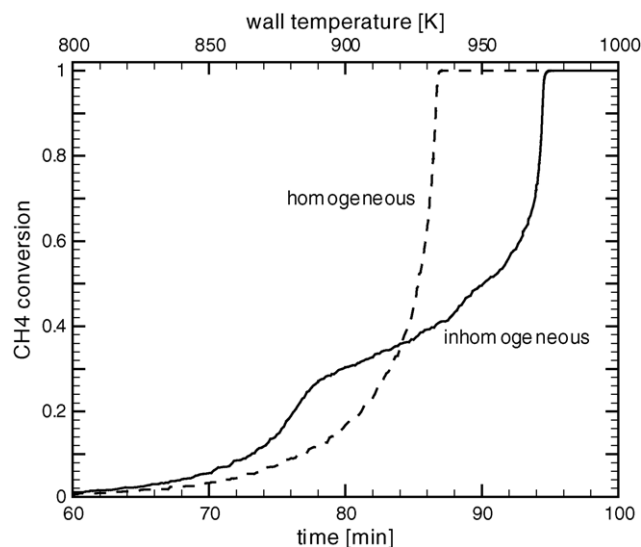


Fig. 4. Global methane conversion as function of time (or corresponding wall temperature) for homogeneous and inhomogeneous velocity inlet profiles.

The monolith is heated from outside. First, ignition occurs in the channels with low mass flow near the exit. Until $t = 90$ min, the hottest spots are in these channels. The cooling of the high mass flow channels still dominates. Once ignition occurs in these channels, the reaction front travels to the front of the monolith within seconds. After 100 min, the hottest zones are at the entrance of these channels.

5. NO_x storage catalysts

One of the most interesting applications of the code DETCHEM^{MONOLITH} is the automotive catalytic converter. For the reduction of nitrogen oxide emissions of lean operated internal combustion engines, the currently most promising system is the NO_x storage catalysts containing barium compounds as storage material [6–9]. Although many experimental studies have recently been conducted for storage catalysts, there is only few data available on the details of the chemical reaction mechanism. DETCHEM^{MONOLITH} is exemplarily applied here to study NO_x storage catalysts numerically.

Olsson et al. [6] suggested a mechanism involving platinum and barium oxide as the active surfaces. However, this mechanism was formulated in a way that does not look at the catalyst as a surface, but as some porous medium interacting with the exhaust gas with its entire volume. Converting the amount of catalyst into parameters for catalytic surface area turned out to be difficult and is not independent of the dispersion.

Therefore, we here chose a five step global reaction mechanism proposed by Tuttlies et al. [9], which involves reactions on platinum and barium carbonate. The oxidation of NO to NO₂ and reduction of NO with carbon monoxide is

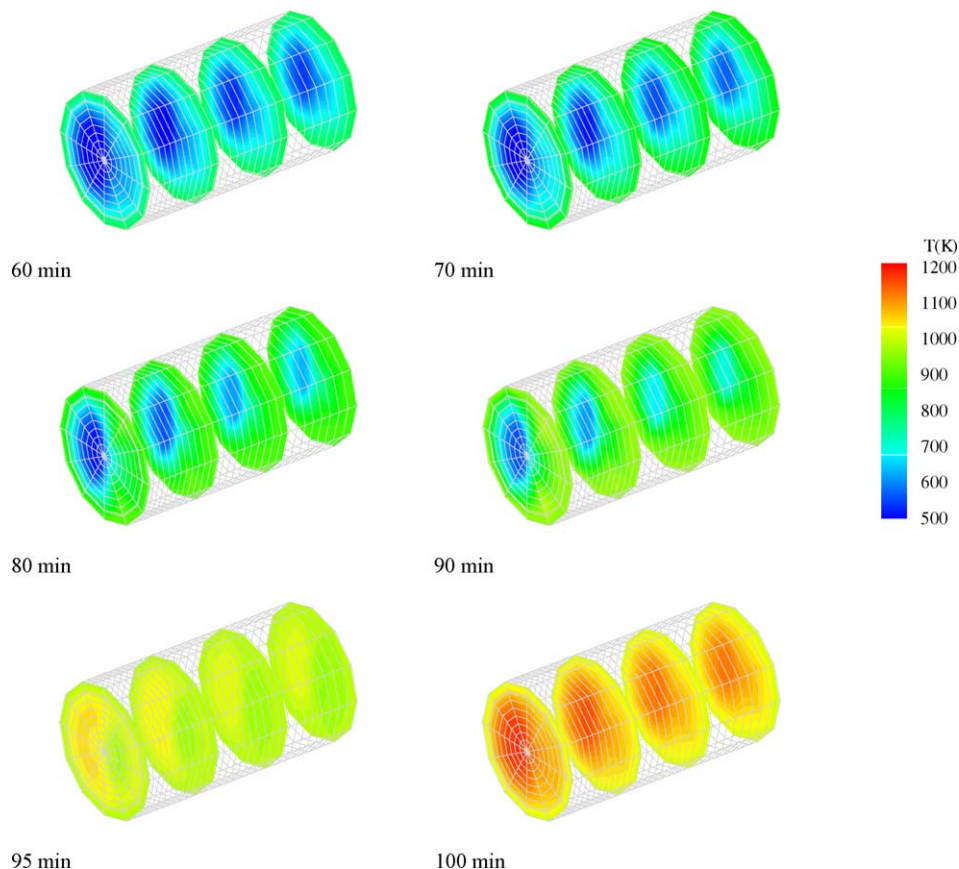


Fig. 5. Temperature profiles of the monolith with inhomogeneous inlet velocity. (The monolith axis has been enlarged by a factor of 5 for viewing.)

assumed to take place on platinum surfaces. Under fuel lean conditions, NO_2 is stored as barium nitrate. The NO_x is released under fuel rich conditions when carbon monoxide can replace the nitrate by carbonate.

For this numerical study, the reaction rate coefficients and the active surface area for the barium reactions have been estimated to display an experimentally observed behaviour of storing and regeneration. The process is driven in cycles with phases of lean fuel/air mixtures (200 ppm NO, 40 ppm NO_2 , 400 ppm CO, 12% O_2) for 60 s and rich mixtures (200 ppm NO, 40 ppm NO_2 , 2.1% CO, 0.9% O_2) for 5 s. These time varying inlet conditions were applied in a one-

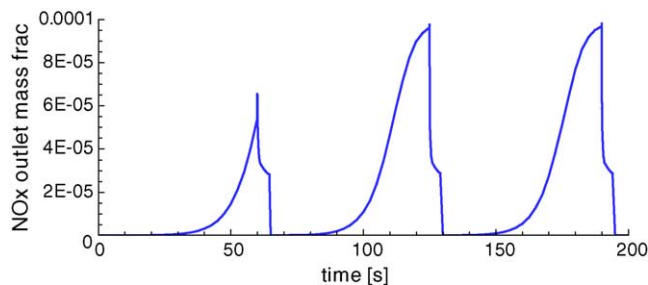


Fig. 6. NO_x outlet mass fractions of a storage catalyst for three lean/rich cycles (60/5 s).

dimensional model of a monolith with storage species barium carbonate and barium nitrate. The monolith length is 20 cm. The reactor was operated isothermal at 350 °C.

The resulting NO_x mass fractions at the outlet of the monolith are shown in Fig. 6. This fairly simple mechanism

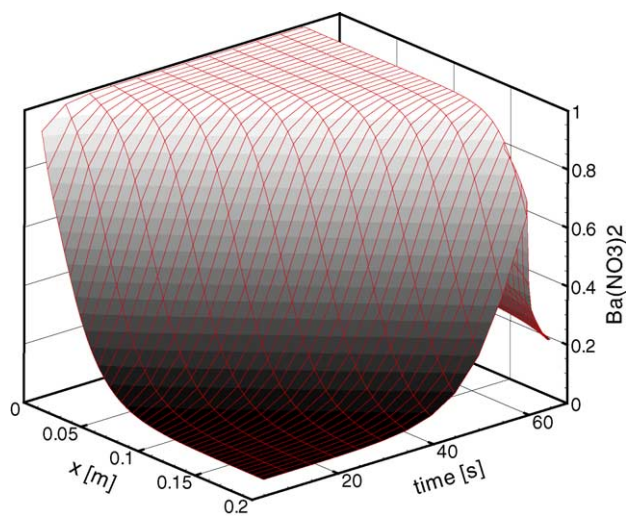


Fig. 7. $\text{Ba}(\text{NO}_3)_2$ coverage as function of position and time for one lean/rich cycle.

is capable of displaying the main properties of storage catalysts. During the first 60 s of storing, the NO_x breakthrough increases steadily. When switching the inlet composition, there is a peak concentration of NO_x observable. In the regeneration phase the emission is decreased slowly, leaving enough storage sites for the next cycle. However, with the chosen parameters, regeneration was not complete, so that the maximum storage capacity is reached before switching to fuel rich conditions.

The concentration of the stored barium nitrate as function of the position inside the reactor for the first cycle is shown in Fig. 7. It can be clearly seen how the storage medium fills up from the front to the back and the sharp drop of the concentration on regeneration.

6. Conclusions

The numerical studies presented in this paper can be seen as examples for a wide variety of problems in application of structured catalysts. The program DETCHEM^{MONOLITH} can be used whenever the interactions of chemistry, transport and reactor properties shall be investigated in monolithic structures of straight channels. The newly developed algorithms allow simulations with a high degree of details with a reasonable computational effort.

The tool is ready to use for systems with well understood detailed kinetics, such as catalytic combustion over noble metals, but also lumped kinetics. One major application is in the field of reactor design studies, for instance to answer the question how the geometry influences the reactor performance. In the field of automotive catalytic converters, the importance of numerical simulations is currently increasing rapidly. One of the main issues for these reactors is the development of detailed reaction mechanisms. Proposed mechanisms can be evaluated by numerical simulation of the entire converter under technical conditions, for instance, an entire driving test cycle can be simulated [19]. Thus, the computational tools developed will help to understand the molecular processes as well as assist in reactor design and optimization.

Acknowledgement

Financial support by the Deutsche Forschungsgemeinschaft (DFG) under contract number DE 659/3-1 is gratefully acknowledged.

References

- [1] S. Tischer, C. Correa, O. Deutschmann, *Catal. Today* 69 (2001) 57–62.
- [2] R.E. Hayes, L.S. Muhadi, M. Votsmeier, J. Gieshoff, *Top. Catal.* 30/31 (2004) 411–415.
- [3] P. Koci, M. Kubicek, M. Marek, *Ind. Eng. Chem. Res.* 43 (2004) 4503–4510.
- [4] K. Ramanathan, D.H. West, V. Balakotaiah, *Ind. Eng. Chem. Res.* 43 (2004) 4668–4690.
- [5] G.N. Pontikakis, G.S. Konstantas, A.M. Stamatelos, *J. Eng. Gas Turb. Power* 126 (2004) 906–923.
- [6] L. Olsson, H. Persson, E. Fridell, M. Skoglundh, B. Andersson, *J. Phys. Chem. B* 105 (2001) 6895–6906.
- [7] P. Broqvist, H. Grönbeck, E. Fridell, I. Panas, *Catal. Today* 96 (2004) 71–78.
- [8] A. Scotti, I. Nova, E. Tronconi, L. Castoldi, L. Lietti, P. Forzatti, *Ind. Eng. Chem. Res.* 43 (2004) 4522–4534.
- [9] U. Tuttlies, V. Schmeißer, G. Eigenberger, *Top. Catal.* 30/31 (2004) 187–192.
- [10] R. Carroni, T. Griffin, I. Mantzaras, M. Reinke, *Catal. Today* 83 (2003) 157–170.
- [11] O. Deutschmann, S. Tischer, et al. DETCHEM 2.0, <http://www.detchem.com>.
- [12] R.J. Kee, M.E. Coltrin, P. Glarborg, *Chemically Reacting Flow Theory & Practice*, Wiley-Interscience, 2003.
- [13] P. Deuffhardt, E. Hairer, J. Zugk, *Numerische Mathematik* 51 (1987) 501–516.
- [14] A.K. Jain, M.N. Murty, P.J. Flynn, *ACM Comput. Surv.* 31 (3) (1999) 264–323.
- [15] J. Warnatz, U. Maas, R.W. Dibble, *Combustion*, third ed., Springer, Heidelberg, 2001.
- [16] O. Deutschmann, R. Schmidt, F. Behrendt, J. Warnatz, *Proc. Combust. Inst.* 26 (1996) 1747–1754.
- [17] D.N. Tsinoglou, G.C. Koltsakis, D.K. Missirlis, K.J. Yakinthos, *Appl. Math. Model.* 28 (2004) 775–794.
- [18] A.P. Martin, N.S. Will, A. Bordet, P. Cornet, C. Gondoin, X. Mouton, SAE 98-0936.
- [19] J. Braun, T. Hauber, H. Többen, J. Windmann, P. Zacke, D. Chatterjee, C. Correa, O. Deutschmann, L. Maier, S. Tischer, J. Warnatz, SAE 2002-01-0065.